Int J Clin Exp Med 2019;12(4):3430-3439
www.ijcem.com /ISSN:1940-5901/IJCEM0089195

*Original Article*

# Identification of molecular target genes and key pathways in nasopharyngeal carcinoma by integrated bioinformatic analysis

Zhong-Guo Liang[1*], Ye Li[1*], Yu-Feng Lv[2], Ding-Jian Liang[1], Ren-Ba Liang[1], Chun-Qiu Lin[3], Yan-Xia Dai[3], Xiao-Dong Zhu[1]

*[1]Department of Radiation Oncology, The Affiliated Tumor Hospital of Guangxi Medical University, Cancer Institute of Guangxi Zhuang Autonomous Region, 71 Hedi Road, Nanning 530021, Guangxi, China; [2]Department of Medical Oncology, Affiliated Langdong Hospital of Guangxi Medical University, 60 Xiangbin Road, Nanning 530021, Guangxi, China; [3]Department of General Medicine, Guangxi Medical University, 22 Shuangyong Road, Nanning 530021, Guangxi, China. [*]Equal contributors and co-first authors.*

Received November 30, 2018; Accepted January 8, 2019; Epub April 15, 2019; Published April 30, 2019

**Abstract:** Purpose: The current study aims to identify potent molecular target genes and key pathways involving the occurrence, development, and prognosis of nasopharyngeal carcinoma (NPC), and highlight their critical roles in management of NPC. Materials and methods: Expression profiling data for patients with NPC and non-cancer were searched and downloaded from the database of Gene Expression Omnibus. The data sets were applied to identify differentially expressed genes (DEGs) between the NPC group and the non-neoplastic group using the linear models for microarray analysis (limma) package in R language. Function enrichment analyses of DEGs wasperformed. The protein-protein interaction network was constructed and analyzed using String and Cytoscape, allowing the identification of hub genes for further analysis. Results: We identified 190 DEGs, of which 69 were upregulated and 121 genes were downregulated in NPC tissues compared to non-tumor tissues. Gene ontology enrichment analysis revealed that DEGs were mainly enriched in leukocyte migration, T cell activation, and cell adhesion. Kyoto Encyclopedia of Genes and Genomes pathway analysis indicated that the DEGs were mainly involved in nuclear factor-kappa B signalling pathway. Twenty hub genes were identified in the PPI network, including 5 up-regulated genes (FN1, PTGS2, CCND1, ITGAV, and STAT1), and 15 down-regulated genes (LCK, CD19, CCR7, ZAP70, RAC2, CD22, SELL, CD48, PTPN6, TNFRSF13C, BTK, CCL21, PLCG2, TNFSF11, and GNG7). Conclusion: Potential target genes and pathways were screenedvia integrated bioinformatic analysis. Future work is essential to verify the function of them across molecular biological experiments.

**Keywords:** Nasopharyngeal carcinoma, target gene, pathway, bioinformatic analysis

## Introduction

Nasopharyngeal carcinoma (NPC) is prevalent in South-Eastern China, Malaysia, Indonesia, Singapore, Eastern Asia, and Northern Africa, with high incidences of 15-50/100,000 per year [1, 2]. According to a survey from the International Agency for Research on Cancer, there was an estimated 86,700 new cases and 50,800 related deaths in 2012 [2]. Patients with NPC are relatively asymptomatic at early stage as they originate in nasopharyngeal cavity, and therefore patients are often diagnosed with advanced disease when nodal metastasis occurs, or the tumor involves the adjacent critical normal structures like medial/lateral pterygoid, skull base, and the optic nerve. Though multidisciplinary approaches including radiotherapy, chemotherapy, and target therapy have been utilized, outcomes of these patients remain unsatisfactory, with relatively high rates of 5-year distant metastasis (15-21%) [3-5]. Therefore, it is worthwhile to identify other potential approaches to optimize survival for NPC.

Recently, microarray technology has become a high-throughput platform and an indispensable

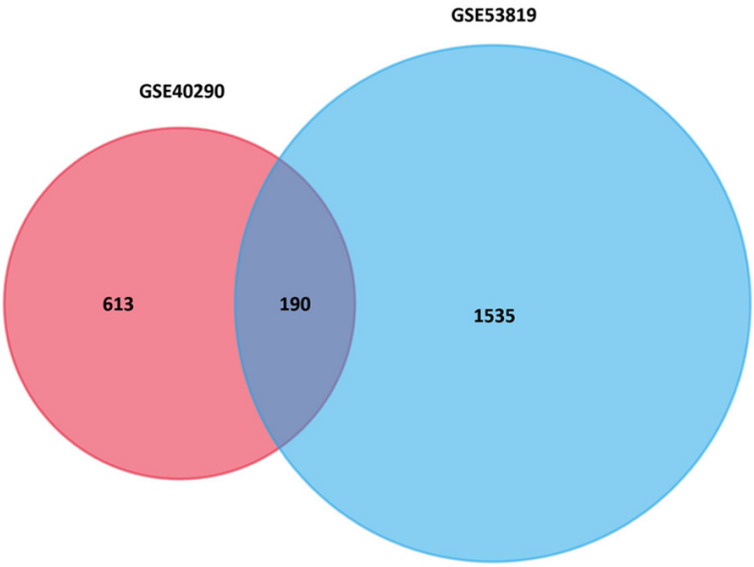


**Figure 1.** Identification of 190 commonly changed DEGs from the two cohort profile data sets (GSE40290, and GSE53819). Different color areas represent different datasets. The cross areas indicate the commonly changed DEGs. DEGs: differentially expressed genes.

tool to detect genome wide expression levels of genes in a given organism. Gene Expression Omnibus (GEO) is a public functional genomics data repository consisting of data from multiple microarray platforms [6]. Bioinformatics analysis has allowed for comprehensive identification of hundreds of differentially expressed genes (DEGs), molecular pathways, and complex interaction network involved in the tumorigenesis, development, and progression of cancers. In the present study, potent molecular target genes and key pathways are demonstrated involving the occurrence, development, and prognosis of NPC, and their critical roles in management of NPC are highlighted.

## Materials and methods

### *Microarray data and Identification of DEGs*

Two gene expression profiles (GSE40290, and GSE53819) were downloaded from the database of GEO (https://www.ncbi.nlm.nih.gov/geo/). The array data of GSE40290 included 25 primary non-keratinizing NPCs and 8 nasopharyngitis tissues, based on the GPL8380 Capitalbio 22K Human oligo array version 1.0 platform (Capitalbio. Crop, Beijing, China). GSE53819 consisted of 18 NPC tissue samples and 18 non-cancerous nasopharyngeal tissues, based on the GPL6480 Agilent-014850 Whole Human Genome Microarray 4x44K G4112F platform (Agilent Technologies, Palo Alto, CA, USA). Given the genes corresponded to several probes, the average expression values of these probes were calculated to determine the expression value of the gene. Subsequently, the skewed distribution of data was converted into a normal distribution using a log 2 transformation, followed by normalization using the Median method [7]. The Linear Models for Microarray Analysis (limma) package [8] in R language was used to screen for the DEGsbetween the NPC and non-NPC tissue samples. |log2 Fold Change|>1 and *P* value <0.01 were set as the strict cut-offs for DEG identification. Bidirectional hierarchical clustering was applied to DEGs based on Euclidean distance and displayed the results as a heat map.

### *Gene ontology and pathway enrichment*

With the implementation of the R package of "clusterProfiler" methods [9], the functional profiles of gene and gene clusters were performed, including gene ontology (GO) [10] and Kyoto Encyclopedia of Genes and Genomes (KEGG) pathway enrichment [11]. GO analyses included cell component (CC), biological process (BP) and molecular function (MF). A false discovery rate (FDR) <0.05 were considered significant.

### *Protein-protein interaction (PPI) network analysis*

PPI network can help us obtain insights into interactions among DEGs, which correlate with oncogenesis, development and prognosis of NPC. The related information was gained by Search Tool for the Retrieval of Interacting Genes (STRING; http://string-db.org). An interaction with a combined score ≥0.4 was considered statistically significant. Then, a PPI network was constructed by Cytoscape software [12]. Moreover, cytoHubba, as a plugin of Cytoscape software [13], was employed to calculate

**Table 1.** Common differentially expressed genes identified in nasopharyngeal carcinoma

| Regulation | Differentially expressed genes (gene symbol) |
|---|---|
| Up-regulated | POSTN, HOXA9, AQP9, TNFAIP6, PTGS2, KREMEN2, FN1, COL17A1, COL4A5, MMP3, ARNT2, ZNF488, PTK7, PLAU, CXADR, PCSK6, RCN1, HOXA10, DIAPH3, COL5A1, LRP4, NRXN1, GPC1, ASB9, NFE2L3, PTPRF, RBBP8, ESM1, WBP5, TUFT1, GPR143, SNAI2, ITGAV, EPHB4, KCTD3, GRB10, SOX4, VRK2, PLXNA1, FOXM1, PFKFB4, C5 or f13, MPP3, CENPF, IGSF3, ADAM9, RGS20, SPR, LAMB1, CCND1, CLDN12, GALNT11, HOMER1, ABTB2, PLAUR, ZIC2, STAT1, MYO10, DSCAM, RAI14, DSG2, PRC1, TK1, IDH1, COL7A1, ITPKA, TFAP2C, CIT, ANXA4 |
| Down-regulated | LTF, BLK, RBP5, PTGDS, CCL21, CD19, VPREB3, SCGB1A1, DHRS9, PTPN6, CD72, SELL, MS4A1, ADRA2A, CD37, FOXJ1, TIMD4, PTPRCAP, KRT4, SLC27A6, KLF2, CCR7, DPT, RASGRP2, ADCY4, MSMB, UPK1B, CR2, WFDC2, RAB37, MSLN, CNR2, TEKT1, CAPS, CD48, CPNE5, PARVG, CD1C, IL16, CD22, PIGR, SLAMF6, PPP1R16B, RAMP3, ATP2A3, FXYD5, MAP4K1, SELP, HTR3A, TFEB, ATP12A, FAM3D, P2RX5, LY86, CD53, SIDT1, PLCG2, PLA2G10, SERPINB7, BTK, CYP4B1, PSD4, CARD11, NFATC1, TNFRSF13C, TCF7, ARHGAP9, RARRES2, RRAD, OSBPL10, TNFRSF13B, P2RY14, MFAP4, STAG3, POU2AF1, GNG7, LRMP, CYP2F1, DPEP2, KLRB1, CHI3L2, SP140, FOLR2, FCER2, EFHC2, SIPA1, FGD3, KIF9, MEF2C, CDH26, SPATS1, FRZB, EVI2B, MFNG, LCK, HOXA2, RAC2, TREML2, ARHGEF1, FIGF, KCNK12, TNFSF11, PLEKHB1, CORO1A, C7 or f23, DGKA, SLC9A2, CD1D, WFDC6, ZAP70, APBB1IP, NEIL1, UCP2, GRAP, FILIP1, ARHGAP4, ANGPTL6, LYL1, TRAF5, C22 or f23, HRASLS2 |

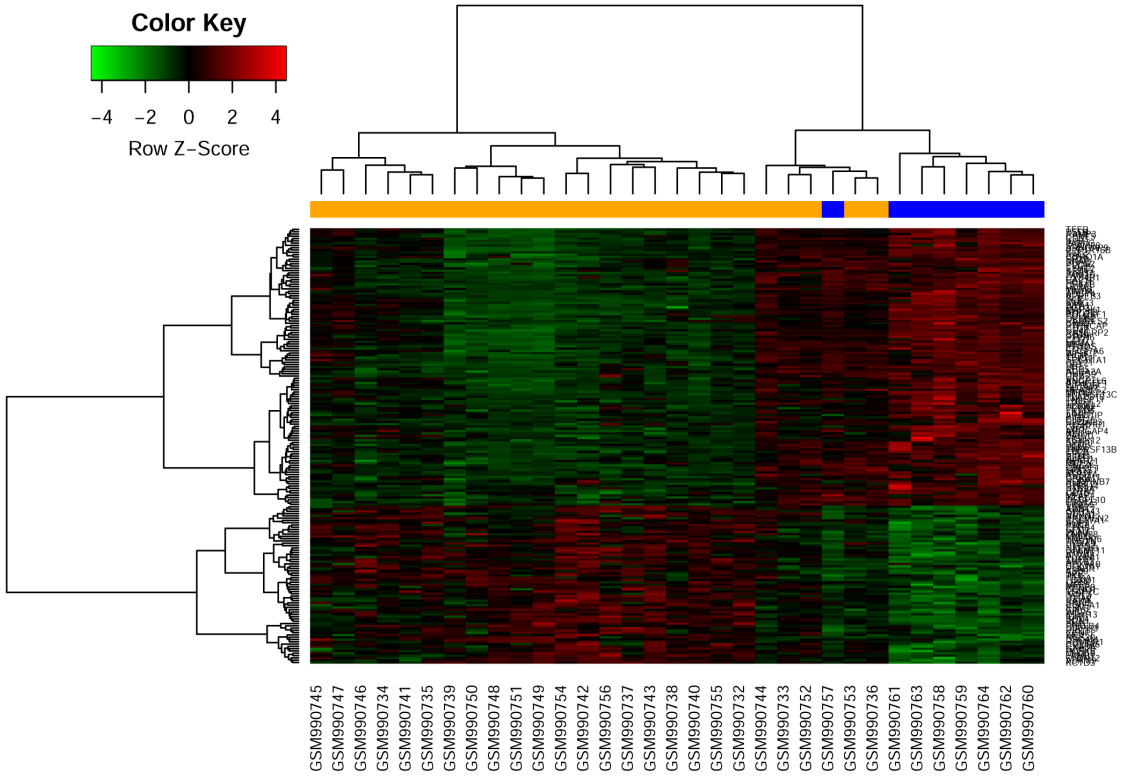


**Figure 2.** Heat map of the DEGs with fold change >2 from the GSE40290 data sets. Red: up-regulated DEGs; Green: down-regulated DEGs.

the node degree, and the number of inter-connections to screen the hub genes of PPI. The top twenty genes selected by degree algorithm [14] were defined as hub genes. Finally, the PPI network of hub genes was constructed by Cytoscape software [12].

## Results

### *Identification of DEGs*

In total, 803 and 1725 DEGs were respectively identified from GSE40290, and GSE53819

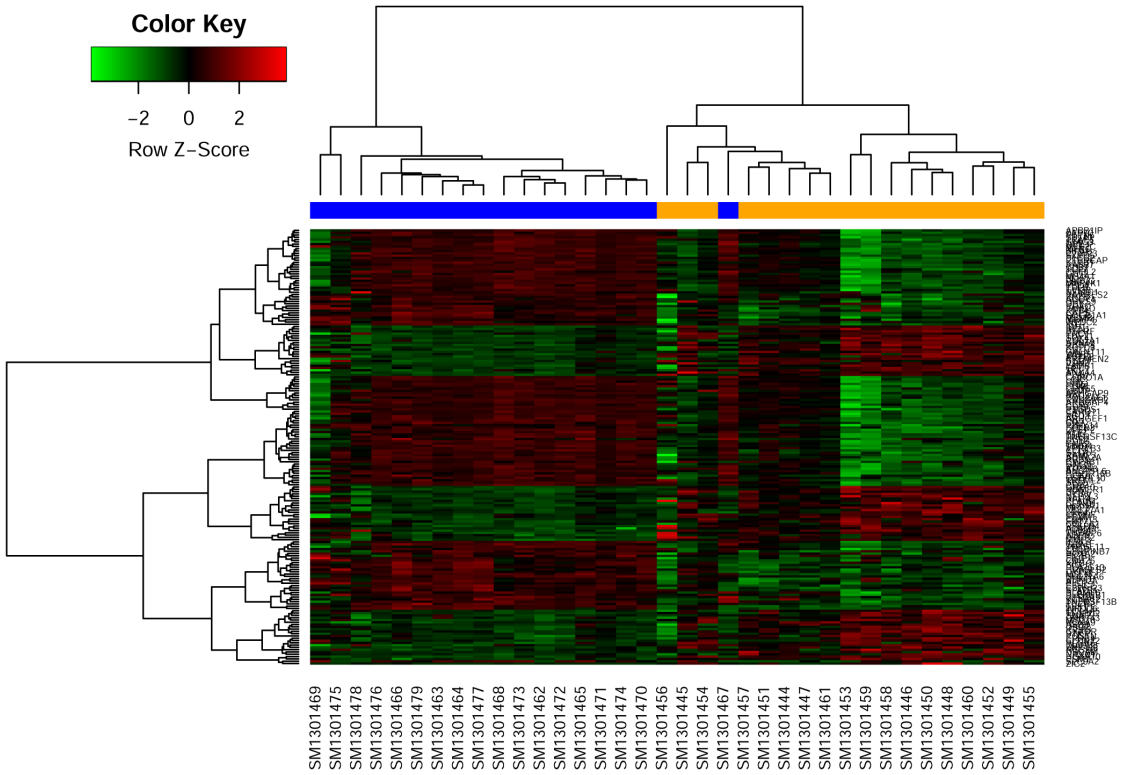


**Figure 3.** Heat map of the DEGs with fold change >2 from the GSE53819 data sets. Red: up-regulated DEGs; Green: down-regulated DEGs.

datasets, with 190 genes screened out in both two datasets (**Figure 1**). Among the 190 genes, 69 were upregulated and 121 genes were downregulated in NPC tissues compared to non-tumor tissues (**Table 1**). In addition, the results of the expression analysis are presented as a heat map (**Figures 2** and **3**), and the results of hierarchical clustering showed these 190 DEGs expression patterns could basically distinguish NPC tissues and non-neoplastic tissues.

*GO and KEGG pathway enrichment analysis*

The annotation of the 190 DEGs was mainly classified into three functional groups: cellular component, biological process and molecular function groups (**Figure 4A-C**). Cellular component analysis revealed that the DEGs were significantly enriched in side of membrane, receptor complex, external side of plasma membrane, plasma membrane receptor complex, and cytoplasmic side of plasma membrane. In terms of biological process, the common DEGs are significantly enriched in leukocyte migration, T cell activation, leukocyte differentiation, leukocyte proliferation, and lymphocyte differentiation. Regarding molecular function, enriched GO terms were mainly cell adhesion molecule binding, sulphur compound binding, glycosaminoglycan binding, and heparin binding. In addition, by KEGG pathway analysis, six significantly enriched pathways were found, including nuclear factor (NF)-kappa B signalling pathway, B cell receptor signalling pathway, proteoglycans in cancer, hematopoietic cell lineage, small cell lung cancer, and primary immunodeficiency (**Figure 4D**).

*Module selection from the PPI network*

Based on the analysis in the STRING database, the PPI network of DEGs was constructed by Cytoscape software. As shown in **Figure 5**, the network consisted of 126 nodes and 277 edges. The pink nodes stand for up-regulated genes, and the green nodes represent down-regulated genes. In addition, twenty hub genes were filtered according to the degree algorithm. Five were up-regulated genes, including FN1,

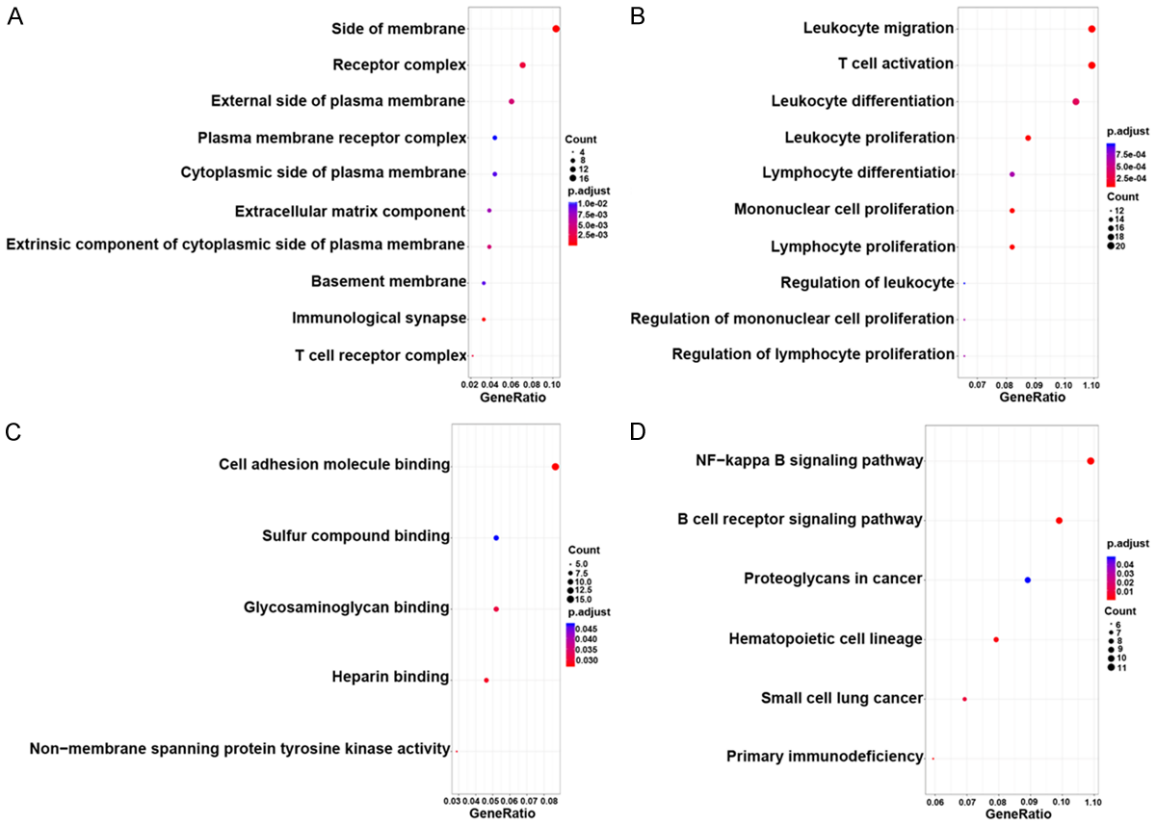


**Figure 4.** Significantly enriched GO annotation and KEGG pathways of differentially expressed genes between nasopharyngeal carcinoma and non-cancer groups. (A) Cellular component, (B) Biological process, (C) Molecular function. (D) KEGG pathway analysis.

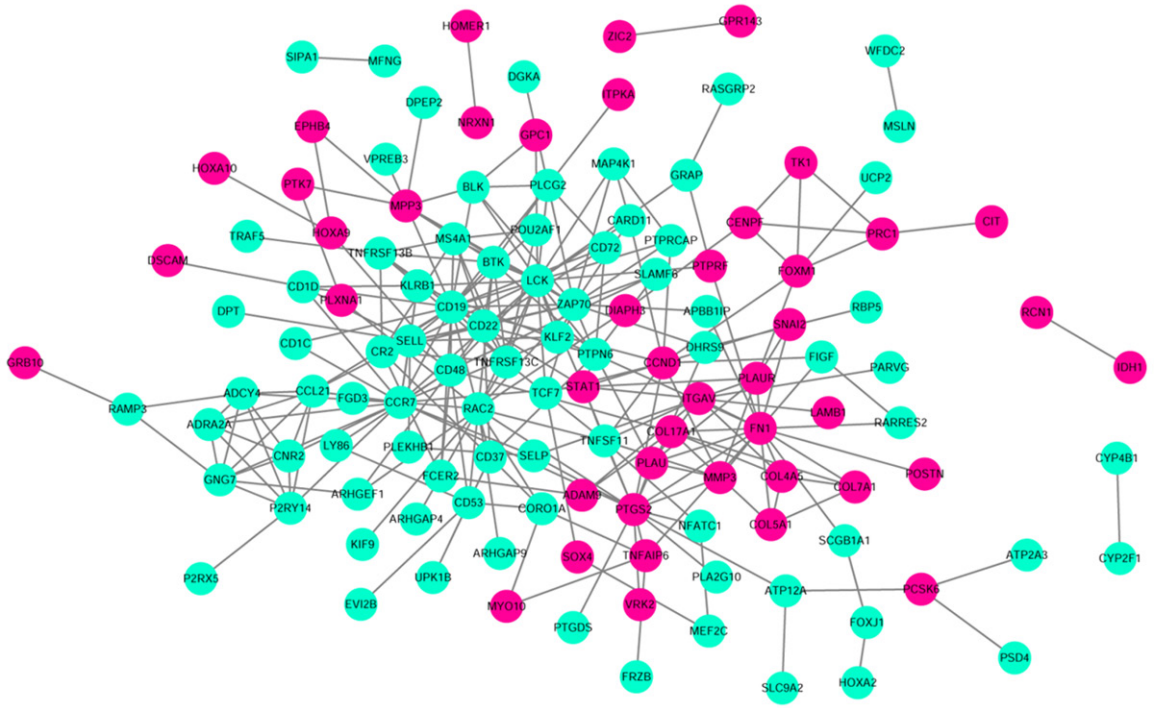

**Figure 5.** PPI Network of DEGs constructed by Cytoscape. The pink nodes stand for up-regulated genes, and the green nodes represent down-regulated genes.

**Table 2.** Twenty hub genes in network string_interactions.tsv ranked by Degree method

| Rank | Gene symbol | Gene description | Score | Regulation |
|---|---|---|---|---|
| 1 | LCK | LCK proto-oncogene | 23 | Down |
| 1 | CD19 | CD19 molecule | 23 | Down |
| 3 | FN1 | Fibronectin 1 | 18 | Up |
| 4 | CCR7 | C-C motif chemokine receptor 7 | 17 | Down |
| 4 | ZAP70 | Zeta chain of T cell receptor associated protein kinase 70 | 17 | Down |
| 6 | PTGS2 | Prostaglandin-endoperoxide synthase 2 | 16 | Up |
| 7 | RAC2 | Rac family small GTPase 2 | 15 | Down |
| 8 | CD22 | CD22 molecule | 12 | Down |
| 8 | SELL | Selectin L | 12 | Down |
| 8 | CD48 | CD48 molecule | 12 | Down |
| 11 | PTPN6 | Protein tyrosine phosphatase, non-receptor type 6 | 11 | Down |
| 11 | CCND1 | Cyclin D1 | 11 | Up |
| 13 | ITGAV | Integrin subunit alpha V | 10 | Up |
| 13 | TNFRSF13C | TNF receptor superfamily member 13C | 10 | Down |
| 15 | BTK | Bruton tyrosine kinase | 9 | Down |
| 15 | STAT1 | Signal transducer and activator of transcription 1 | 9 | Up |
| 17 | CCL21 | C-C motif chemokine ligand 21 | 8 | Down |
| 17 | PLCG2 | Phospholipase C gamma 2 | 8 | Down |
| 17 | TNFSF11 | TNF superfamily member 11 | 8 | Down |
| 17 | GNG7 | G protein subunit gamma 7 | 8 | Down |

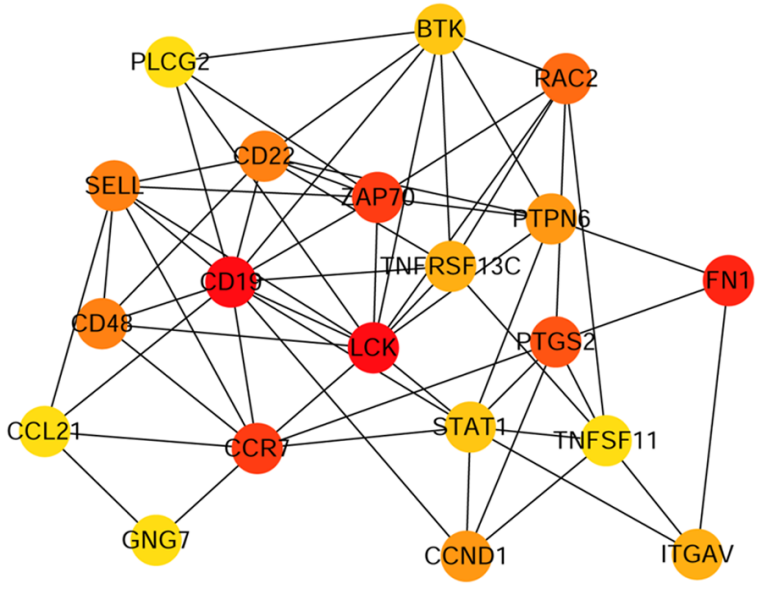


**Figure 6.** PPI Network of twenty hub genes constructed by Cytoscape.

PTGS2, CCND1, ITGAV, and STAT1. Fifteen were down-regulated genes, comprising of LCK, CD19, CCR7, ZAP70, RAC2, CD22, SELL, CD48, PTPN6, TNFRSF13C, BTK, CCL21, PLCG2, TNFSF11, and GNG7. **Table 2** shows the top 20 genes in network string_interactions.tsv ranked by degree method. The PPI Network of the top 20 genes was constructed and visualized by Cytoscape software (**Figure 6**).

## Discussion

In the current cohort, 190 DEGs were identified, including 69 upregulated and 121 downregulated genes between NPC and non-tumor tissues through significant analyses on microarray data. GO enrichment analysis revealed that DEGs were mainly enriched in leukocyte migration, T cell activation, and cell adhesion, which were very associated with tumor growth, invasion, and metastasis [15,

16]. Wang and colleagues observed that that overexpression of epithelial cell adhesion molecule could result in epithelial-mesenchymal transition, stemness, and metastasis of NPC cells [17]. Additionally, targeting of focal adhesion proteins may potently sensitize cancer cells to radiotherapy, and chemotherapy [18].

Pathway enrichment indicated that the DEGs were mainly involved in NF-kappa B signalling pathway. Several studies have reported that this pathway played an important role in the occurrence, progression, and prognosis of several cancers, including prostate cancer [19], colon cancer [20], and head neck cancer [21]. It also correlates with EBV pathogenesis in NPC by regulating BamHI-A rightward transcripts [22]. When the pathway was activated, the radioresistance and chemoresistance could occur in NPC [23, 24]. Correspondingly, inhibition of the pathway might bring good anticancer results via inducing G2/M phase arrest and apoptosis [25]. Therefore, it may be a potential target pathway for improving therapeutic effects. More evidence is needed in this regard to confirm the efficacy of targeting this pathway in vivo and vitro.

By establishing a PPI, twenty hub genes were screened, which would provide new insights for NPC intervention strategy. FN1 is a member of the glycoprotein family, which involves in cell adhesion and migration processes [26, 27] that could promote cell proliferation and metastases by facilitating epithelial-mesenchymal transition (EMT) process of NPC cells [28]. Another mechanism has been reported that FN1 could inhibit apoptosis by upregulating BCL2, and promote migration and invasion [29]. In addition, expression of FN1 is negatively related to the prognosis of NPC including distant metastasis-free survival, and local recurrence-free survival [30]. Therefore, FN1 may be a potent therapeutic target for the treatment of NPC.

PTGS-2, also known as Cyclooxygenase-2 (COX-2), is the key enzyme in prostaglandin biosynthesis, and acts both as a dioxygenase and as a peroxidase. Overexpression of COX-2 was significantly found in patients with NPC. High level of its expression might contribute to a poor prognosis for NPC [31, 32]. First, high expression of COX-2 is related to high risk of lymph node metastasis [32], which has been proven to be an independent poor prognosis factor. Second, higher levels of COX-2 would result in increasing cell proliferation, and suppression of cellular senescence via the inactivation of p53, resulting in chemoresistance [31]. Moreover, it had been demonstrated that the expression of mitochondrial COX-2 would promote the stemness of NPC [33].

The protein encoded by CCND1 belongs to the highly conserved cyclin family. Wong and colleagues demonstrated that CCND1 was overexpressed in over 90% of NPC, and its activation played a critical role in NPC pathogenesis [34]. In addition, it might be an important target in regulating NPC cell cycle. It was observed that ribociclib, a specific cyclin dependent kinase (Cdk) 4/6 inhibitor, could lead to G1 arrest by blocking the formation of cyclin D1-Cdk4/6 complex [34]. It also appears that CCND1 isone of the crucial links in the process of regulating cell cycle for several micro-RNAs and long noncoding RNAs (lncRNAs), including miR-374a, miR-150, and lncRNA AK294004 [35-37]. For example, miR-374a could directly target CCND1 to inactivate pPI3K/pAKT/c-JUN forming a negative feedback loop, as well as suppressing downstream signals related to cell cycle progression and epithelial-mesenchymal transition (EMT), which would suppress NPC cell growth, metastasis and sensitizes NPC to cisplatin [35]. Additionally, lncRNA AK294004 could enhance radiation sensitivity via a negative effect on CCND1 [37]. Consequently, it seems promising to perform trials to investigate whether the target for CCND1 can translate to superior survival by improving radiosensitivity, and reducing metastasis for NPC.

The protein encoded by STAT1 is a member of the STAT protein family. Several evidences have shown Inhibition of STAT1 might help relieve immune tolerance in NPC by suppressing the expression of indoleamine 2,3-dioxygenase, which is a molecule of immune tolerance via decreasing T-cell proliferation. Furthermore, STAT1 may be closely associated with radiation resistance for NPC. Compared to CNE-2, significant higher expression of STAT1 was reported in CNE-2R, a radioresistant cell line [38]. Inhibition of STAT1 could enhance radiosensitivity of CNE-2R by increasing the proportion of G2/M phase, suppressing growth, and promoting apoptosis *in vitro* and *in vivo* [39]. Hence, it

may be an optimal therapeutic target for radioresistant NPC.

Various studies have shown that CD19 plays an important role in diagnosis and prognosis for NPC. First, the percentage of $CD19^+$ circulating lymphocytes correlated negatively with TNM stage of NPC [40]. Secondly, after radiotherapy and chemotherapy, the percentage of $CD19^+$ lymphocytes significantly decreased in NPC patients [40]. Moreover, patients with high circulating $CD19^+$ B cell possessed significant better 5-year progression-free survival (PFS) than those with low circulating $CD19^+$ B cell (81.8% vs. 66.6%, P=0.036) [41]. However, the mechanism is unclear why the level of $CD19^+$ lymphocytes influences the long term survival of NPC.

PTPN6, also known as Src homology region 2 domain-containing phosphatase-1 (SHP-1). A dataset has shown that SHP-1 is negatively associated with radiation sensitivity for NPC. The mechanism may be that SHP-1 overexpression inhibits cellular senescence, enhance DNA DSB repair, increase S phase arrest and decrease cell apoptosis [42]. These were consistent with clinical observations by Peng et al. who observed high expression of SHP-1 was significantly associated with poor local recurrence-free survival [43] (P=0.008).

In conclusion, key target genes and pathways were screened via integrated bioinformatic analysis, which involved in the initiation, development, and progression of NPC. Given their potential roles in targeting NPC, future work is essential to verify the function of them across molecular biological experiments to enhance therapeutic outcomes.

## Acknowledgements

This work was sponsored by the Basic Ability Enhancement Project of Young Teachers in Guangxi Zhuang Autonomous Region (2017-KY0114, 2017), the Youth Science Foundation of Guangxi Medical University (GXMUYSF201515, 2015), and International Communication of Guangxi Medical University Graduate Education in 2018.

## Disclosure of conflict of interest

None.

**Address correspondence to:** Dr. Xiao-Dong Zhu, The Affiliated Tumor Hospital of Guangxi Medical University, 71 Hedi Road, Nanning 530021, Guangxi, China. Tel: 86-771-5331466; E-mail: zhuxdonggxmu@126.com

## References

[1] Petersson F. Nasopharyngeal carcinoma: a review. Semin Diagn Pathol 2015; 32: 54-73.

[2] Torre LA, Bray F, Siegel RL, Ferlay J, Lortet-Tieulent J and Jemal A. Global cancer statistics, 2012. CA Cancer J Clin 2015; 65: 87-108.

[3] Wang F, Sun Q, Jiang C, Liu T, Rihito A, Masoto S, Wang Y, Fu Z and Chen M. Additional induction chemotherapy to concurrent chemotherapy and intensity-modulated radiotherapy with or without nimotuzumab in first-line treatment for locoregionally advanced nasopharyngeal carcinoma: a propensity score matched analysis. J Cancer 2018; 9: 594-603.

[4] Chen L, Hu CS, Chen XZ, Hu GQ, Cheng ZB, Sun Y, Li WX, Chen YY, Xie FY, Liang SB, Chen Y, Xu TT, Li B, Long GX, Wang SY, Zheng BM, Guo Y, Sun Y, Mao YP, Tang LL, Chen YM, Liu MZ and Ma J. Adjuvant chemotherapy in patients with locoregionally advanced nasopharyngeal carcinoma: long-term results of a phase 3 multicentre randomised controlled trial. Eur J Cancer 2017; 75: 150-158.

[5] Xu T, Zhu G, He X, Ying H and Hu C. A phase III randomized study comparing neoadjuvant chemotherapy with concurrent chemotherapy combined with radiotherapy for locoregionally advanced nasopharyngeal carcinoma: updated long-term survival outcomes. Oral Oncol 2014; 50: 71-76.

[6] Parkinson H, Kapushesky M, Shojatalab M, Abeygunawardena N, Coulson R, Farne A, Holloway E, Kolesnykov N, Lilja P, Lukk M, Mani R, Rayner T, Sharma A, William E, Sarkans U and Brazma A. Arrayexpress--a public database of microarray experiments and gene expression profiles. Nucleic Acids Res 2007; 35: D747-750.

[7] Fujita A, Sato JR, Rodrigues Lde O, Ferreira CE and Sogayar MC. Evaluating different methods of microarray data normalization. BMC Bioinformatics 2006; 7: 469.

[8] Ritchie ME, Phipson B, Wu D, Hu Y, Law CW, Shi W and Smyth GK. limma powers differential expression analyses for RNA-sequencing and microarray studies. Nucleic Acids Res 2015; 43: e47.

[9] Yu G, Wang LG, Han Y and He QY. clusterprofiler: an R package for comparing biological themes among gene clusters. OMICS 2012; 16: 284-287.

[10] Torto-Alalibo T, Purwantini E, Lomax J, Setubal JC, Mukhopadhyay B and Tyler BM. Genetic resources for advanced biofuel production described with the gene ontology. Front Microbiol 2014; 5: 528.
[11] Kanehisa M. The KEGG database. Novartis Found Symp 2002; 247: 91-101.
[12] Shannon P, Markiel A, Ozier O, Baliga NS, Wang JT, Ramage D, Amin N, Schwikowski B and Ideker T. Cytoscape: a software environment for integrated models of biomolecular interaction networks. Genome Res 2003; 13: 2498-2504.
[13] Chin CH, Chen SH, Wu HH, Ho CW, Ko MT and Lin CY. cytoHubba: identifying hub objects and sub-networks from complex interactome. BMC Syst Biol 2014; 8 Suppl 4: S11.
[14] Jeong H, Mason SP, Barabasi AL and Oltvai ZN. Lethality and centrality in protein networks. Nature 2001; 411: 41-42.
[15] Caronni N, Savino B, Recordati C, Villa A, Locati M and Bonecchi R. Cancer and chemokines. Methods Mol Biol 2016; 1393: 87-96.
[16] Jacquemet G, Hamidi H and Ivaska J. Filopodia in cell adhesion, 3D migration and cancer cell invasion. Curr Opin Cell Biol 2015; 36: 23-31.
[17] Wang MH, Sun R, Zhou XM, Zhang MY, Lu JB, Yang Y, Zeng LS, Yang XZ, Shi L, Xiao RW, Wang HY and Mai SJ. Epithelial cell adhesion molecule overexpression regulates epithelial-mesenchymal transition, stemness and metastasis of nasopharyngeal carcinoma cells via the PTEN/AKT/mTOR pathway. Cell Death Dis 2018; 9: 2.
[18] Eke I and Cordes N. Focal adhesion signaling and therapy resistance in cancer. Semin Cancer Biol 2015; 31: 65-75.
[19] Wang C, Ke Y, Liu S, Pan S, Liu Z, Zhang H, Fan Z, Zhou C, Liu J and Wang F. Ectopic fibroblast growth factor receptor 1 promotes inflammation by promoting nuclear factor-kappaB signaling in prostate cancer cells. J Biol Chem 2018; 293: 14839-14849.
[20] Zhang LL, Mu GG, Ding QS, Li YX, Shi YB, Dai JF and Yu HG. Phosphatase and tensin homolog (PTEN) represses colon cancer progression through inhibiting paxillin transcription via PI3K/AKT/NF-kappaB pathway. J Biol Chem 2015; 290: 15018-15029.
[21] Qin X, Yan M, Wang X, Xu Q, Wang X, Zhu X, Shi J, Li Z, Zhang J and Chen W. Cancer-associated fibroblast-derived IL-6 promotes head and neck cancer progression via the osteopontin-NF-kappa B signaling pathway. Theranostics 2018; 8: 921-940.
[22] Verhoeven RJ, Tong S, Zhang G, Zong J, Chen Y, Jin DY, Chen MR, Pan J and Chen H. NF-kappaB signaling regulates expression of epstein-barr virus BART MicroRNAs and long noncoding RNAs in nasopharyngeal carcinoma. J Virol 2016; 90: 6475-6488.
[23] Li LN, Xiao T, Yi HM, Zheng Z, Qu JQ, Huang W, Ye X, Yi H, Lu SS, Li XH and Xiao ZQ. MiR-125b increases nasopharyngeal carcinoma radioresistance by targeting A20/NF-kappaB signaling pathway. Mol Cancer Ther 2017; 16: 2094-2106.
[24] Kuang CM, Fu X, Hua YJ, Shuai WD, Ye ZH, Li Y, Peng QH, Li YZ, Chen S, Qian CN, Huang W and Liu RY. BST2 confers cisplatin resistance via NF-kappaB signaling in nasopharyngeal cancer. Cell Death Dis 2017; 8: e2874.
[25] Li Y, Qin Y, Yang C, Zhang H, Li Y, Wu B, Huang J, Zhou X, Huang B, Yang K and Wu G. Cardamonin induces ROS-mediated G2/M phase arrest and apoptosis through inhibition of NF-kappaB pathway in nasopharyngeal carcinoma. Cell Death Dis 2017; 8: e3024.
[26] Zollinger AJ and Smith ML. Fibronectin, the extracellular glue. Matrix Biol 2017; 60-61: 27-37.
[27] Erdogan B, Ao M, White LM, Means AL, Brewer BM, Yang L, Washington MK, Shi C, Franco OE, Weaver AM, Hayward SW, Li D and Webb DJ. Cancer-associated fibroblasts promote directional cancer cell migration by aligning fibronectin. J Cell Biol 2017; 216: 3799-3816.
[28] Ding Y, Pan Y, Liu S, Jiang F and Jiao J. Elevation of MiR-9-3p suppresses the epithelial-mesenchymal transition of nasopharyngeal carcinoma cells via down-regulating FN1, ITGB1 and ITGAV. Cancer Biol Ther 2017; 18: 414-424.
[29] Wang J, Deng L, Huang J, Cai R, Zhu X, Liu F, Wang Q, Zhang J and Zheng Y. High expression of fibronectin 1 suppresses apoptosis through the NF-kappaB pathway and is associated with migration in nasopharyngeal carcinoma. Am J Transl Res 2017; 9: 4502-4511.
[30] Ma LJ, Lee SW, Lin LC, Chen TJ, Chang IW, Hsu HP, Chang KY, Huang HY and Li CF. Fibronectin overexpression is associated with latent membrane protein 1 expression and has independent prognostic value for nasopharyngeal carcinoma. Tumour Biol 2014; 35: 1703-1712.
[31] Shi C, Guan Y, Zeng L, Liu G, Zhu Y, Xu H, Lu Y, Liu J, Guo J, Feng X, Zhao X, Jiang W, Li G, Li G, Dai Y, Jin F, Li W and Zhou W. High COX-2 expression contributes to a poor prognosis through the inhibition of chemotherapy-induced senescence in nasopharyngeal carcinoma. Int J Oncol 2018; 53: 1138-1148.
[32] Yang G, Deng Q, Fan W, Zhang Z, Xu P, Tang S, Wang P, Wang J and Yu M. Cyclooxygenase-2 expression is positively associated with lymph node metastasis in nasopharyngeal carcinoma. PLoS One 2017; 12: e0173641.

[33] Zhou TJ, Zhang SL, He CY, Zhuang QY, Han PY, Jiang SW, Yao H, Huang YJ, Ling WH, Lin YC and Lin ZN. Downregulation of mitochondrial cyclooxygenase-2 inhibits the stemness of nasopharyngeal carcinoma by decreasing the activity of dynamin-related protein 1. Theranostics 2017; 7: 1389-1406.

[34] Wong CH, Ma BBY, Hui CWC, Lo KW, Hui EP and Chan ATC. Preclinical evaluation of ribociclib and its synergistic effect in combination with alpelisib in non-keratinizing nasopharyngeal carcinoma. Sci Rep 2018; 8: 8010.

[35] Zhen Y, Fang W, Zhao M, Luo R, Liu Y, Fu Q, Chen Y, Cheng C, Zhang Y and Liu Z. miR-374a-CCND1-pPI3K/AKT-c-JUN feedback loop modulated by PDCD4 suppresses cell growth, metastasis, and sensitizes nasopharyngeal carcinoma to cisplatin. Oncogene 2017; 36: 275-285.

[36] Li X, Liu F, Lin B, Luo H, Liu M, Wu J, Li C, Li R, Zhang X, Zhou K and Ren D. miR150 inhibits proliferation and tumorigenicity via retarding G1/S phase transition in nasopharyngeal carcinoma. Int J Oncol 2017.

[37] Wang Q, Fan H, Liu Y, Yin Z, Cai H, Liu J, Wang Z, Shao M, Sun X, Diao J, Liu Y, Tong L and Fan Q. Curcumin enhances the radiosensitivity in nasopharyngeal carcinoma cells involving the reversal of differentially expressed long noncoding RNAs. Int J Oncol 2014; 44: 858-864.

[38] Guo Y, Zhu XD, Qu S, Li L, Su F, Li Y, Huang ST and Li DR. Identification of genes involved in radioresistance of nasopharyngeal carcinoma by integrating gene ontology and protein-protein interaction networks. Int J Oncol 2012; 40: 85-92.

[39] Qu S, Guo Y, Huang ST and Zhu XD. Inhibition of STAT1 sensitizes radioresistant nasopharyngeal carcinoma cell line CNE-2R to radiotherapy. Oncotarget 2018; 9: 8303-8310.

[40] Hu FJ, Ge MH, Li P, Wang CC, Ling YT, Mao WM and Ling ZQ. Unfavorable clinical implications of circulating CD44+ lymphocytes in patients with nasopharyngeal carcinoma undergoing radiochemotherapy. Clin Chim Acta 2012; 413: 213-218.

[41] Xu T, Huang Z, Su B, Wang S, Wang D, Wang C, Wei W, Jiang J, Zhang G, Yang H and Hu W. Prognostic significance of circulating CD19+ B lymphocytes in EBV-associated nasopharyngeal carcinoma. Med Oncol 2014; 31: 198.

[42] Pan X, Mou J, Liu S, Sun Z, Meng R, Zhou Z, Wu G and Peng G. SHP-1 overexpression increases the radioresistance of NPC cells by enhancing DSB repair, increasing S phase arrest and decreasing cell apoptosis. Oncol Rep 2015; 33: 2999-3005.

[43] Peng G, Cao R, Xue J, Li P, Zou Z, Huang J and Ding Q. Increased expression of SHP-1 is associated with local recurrence after radiotherapy in patients with nasopharyngeal carcinoma. Radiol Oncol 2014; 48: 40-49.